

# Antenna Demonstration System

*Alexander J. Hempy, Michael P. Civerolo, and Dean Y. Arakaki*

## Abstract

This paper describes the design, assembly, and operation of a self-contained wireless demonstration system that required only dc power supplies. The system demonstrated polarization effects, radiation patterns, gain, directivity, and signal interference from environmental barriers for dipole, corner reflector (simulated antenna array), Quagi, and embedded patch antennas. The system included an RF oscillator, high-frequency amplifiers, RF bandpass filters, a signal-strength indicator, and multiple adjustable antenna-mounting platforms.

## Introduction

The antenna demonstration system was designed for ease of use, simple construction, and operation with multiple antenna types. It consisted of four antenna types, a bandpass filter, amplifiers, an oscillator, and a signal-strength detector, as depicted in Figure 1. The system operated at 915 MHz, which allowed for relatively small antennas and eliminated requirements for components that operated at frequencies above UHF.

10 AWG solid copper wire, soldered to the brass tubing. The dipole was fed through an SMA RG174 cable, soldered to the opposite end of the brass-tubing structure.

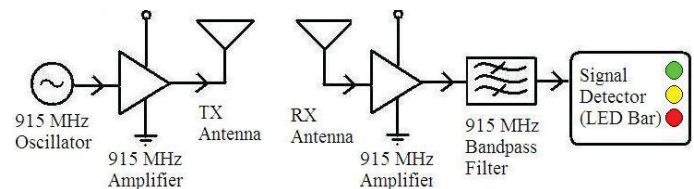


Figure 1. The block diagram for the wireless system.

## 2. System Components

### 2.1 Stationary Dipole Antenna

A stationary dipole antenna was used for 915 MHz signal transmission for all demonstrations (see Figure 2). The stationary dipole was vertically polarized and mounted to a wooden base. The antenna included a 3/8 in brass-tube outer conductor with a 5/32 in brass-tube center conductor. With the selected tube dimensions, Equation (1) yielded a 52.5  $\Omega$  characteristic impedance:

$$Z_0 = 60 \ln(b/a), \quad (1)$$

where  $a$  is the inner-conductor radius and  $b$  is the outer-conductor radius. The dipole incorporated a split-type balun to minimize surface-current radiation. The dipole arms were

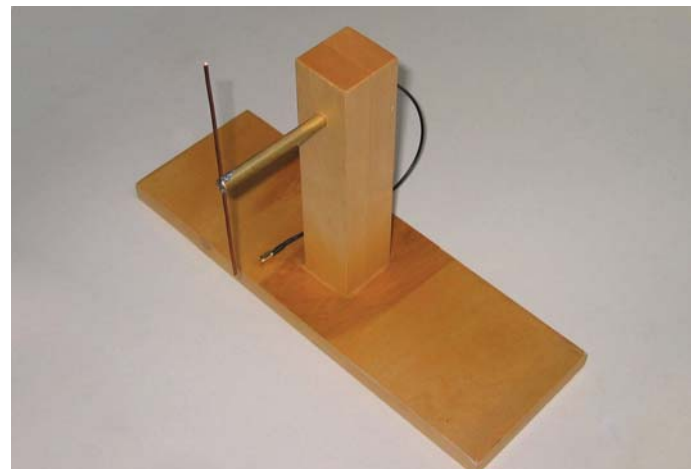


Figure 2. The stationary dipole antenna was used for transmission throughout the entire demonstration

## 2.2 Rotating Dipole Antenna

A rotating dipole, identical to the stationary dipole, was used to demonstrate signal reception (see Figure 3). The polarization effects and radiation-pattern characteristics (including nulls) of the dipole antennas were illustrated.

The rotating dipole antenna was mounted on two lazy Susan bearings to allow rotation in two orthogonal directions: azimuth and roll. These rotational axes were used to illustrate radiation-pattern (received signal strength as a function of angle) and polarization (TX/RX antenna alignment) effects, respectively.

## 2.3 Corner Reflector

A corner reflector was used to demonstrate a simulated dipole antenna array (see Figure 4). The corner reflector included slots positioned for 90°, 60°, and 30° corners that simulated antenna arrays with four, six, and 12 elements, respectively. A dipole antenna identical to the stationary and rotating dipoles was used to receive signals with the corner reflector. The support structure allowed antenna positioning for optimum transmission with different corner angles. The corner reflector was mounted to a lazy Susan, which allowed rotation to demonstrate simulated array radiation patterns.

## 2.4 Quagi Antenna

The Quagi antenna was used to demonstrate directionality and gain. It was a variation of a Yagi-Uda antenna that substituted square loops for dipole elements (see Figure 5). The Quagi antenna had one active element and three parasitic

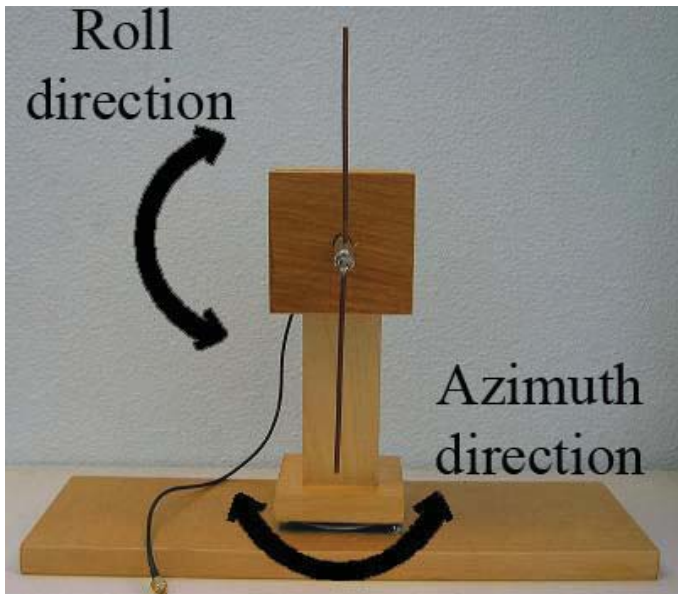


**Figure 3.** A rotating dipole antenna was used to illustrate polarization and radiation-pattern effects.

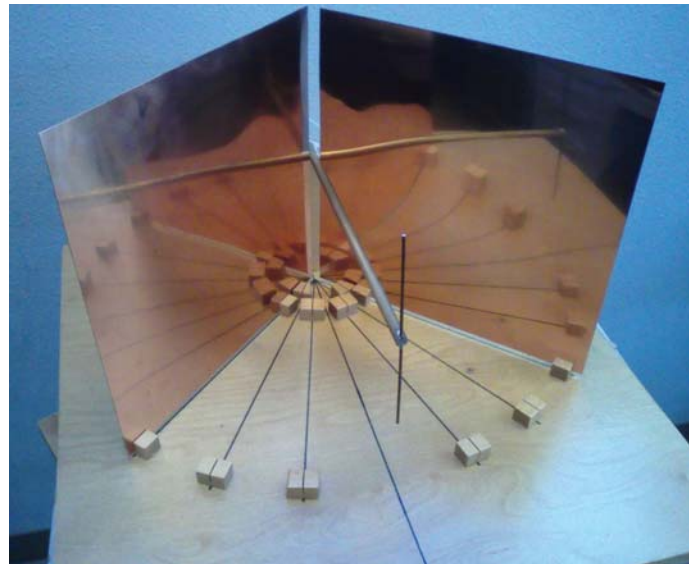


**Figure 4.** The corner reflector antenna simulated an antenna array.

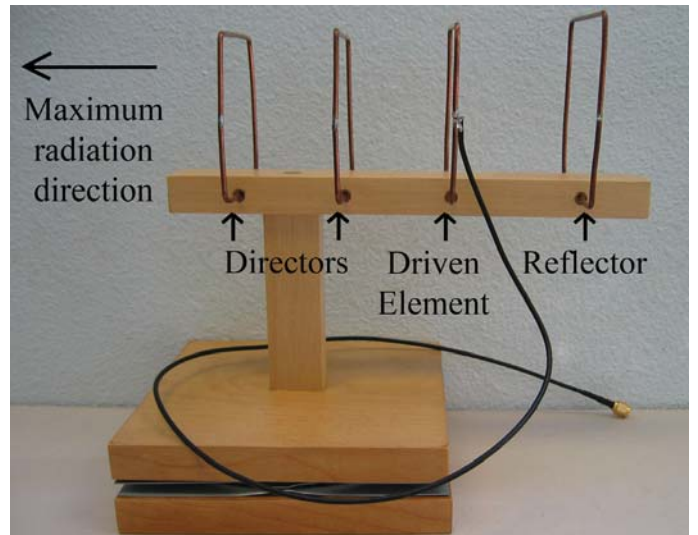


**Figure 5.** The Quagi antenna used parasitic elements to direct the signal from the driven element toward the director elements.

elements: one driven element, one reflector, and two directors. The reflector and director elements focused radiation from the driven element toward the directors. This resulted in a gain (in the maximum-radiation direction) greater than that of a dipole antenna. The Quagi was supported by a wooden boom, positioned above a lazy Susan.

## 2.5 Embedded Printed-Circuit Board Patch Antenna

The embedded printed-circuit board (PCB) patch antenna was used to illustrate a scaled version of current cell-phone antenna technology, and the advantages of a microstrip antenna: low profile, ease of fabrication, low cost, and PCB compatibility

with other circuitry. The patch antenna was milled alongside a 915 MHz amplifier. It was matched to a 50  $\Omega$  transmission line via a quarter-wave transformer (see Figure 6).

## 2.6 Oscillator

A negative-resistance oscillator was used to generate the 915 MHz RF signal. The oscillator provided 0 dBm when supplied with a 9 V dc input. The oscillator coupled energy into a  $\lambda/2$  10 AWG copper-wire resonator to generate oscillations. The oscillator is shown in Figure 7.

## 2.7 Amplifiers

Two amplifiers provided approximately 15 dB gain each: one in the receiver and the other in the transmitter (see Figure 8). The amplifiers were milled on FR4 printed-circuit board. Matching networks minimized reflections and improved amplifier efficiency. High-impedance quarter-wave lines were added to dc bias the high-frequency transistor. The bias lines were ac shorted to ground through coupling capacitors near the biasing circuitry, to create an open circuit at both RF transistor ports.

## 2.8 Bandpass Filters

A second-order coupled-line 915 MHz microstrip bandpass filter suppressed out-of-band reception (see Figure 9). The filter had a nominal 30 MHz 3 dB bandwidth, and approximately 2.7 dB insertion loss at 915 MHz.

## 2.9 Signal-Strength Indicator

The signal-strength detector used an RF peak detector, an LED bar-graph driver, and a gain-adjustable non-inverting operational amplifier (see Figure 10). The peak detector converted the received RF signal to a dc voltage, which was proportional to the received signal strength. This dc voltage was applied to a non-inverting operational amplifier for range adjustment, and to a bar-graph display circuit, which drove a 30-LED array. The number of illuminated LEDs was proportional to the peak detector voltage and the received RF signal strength.

## 2.10 Environmental Barrier

Environmental barriers simulated actual wireless system environments and resultant signal-attenuation effects. The environmental barriers were represented by four 2 ft  $\times$  2 ft frames, composed of drywall, poultry net, ESD material, and

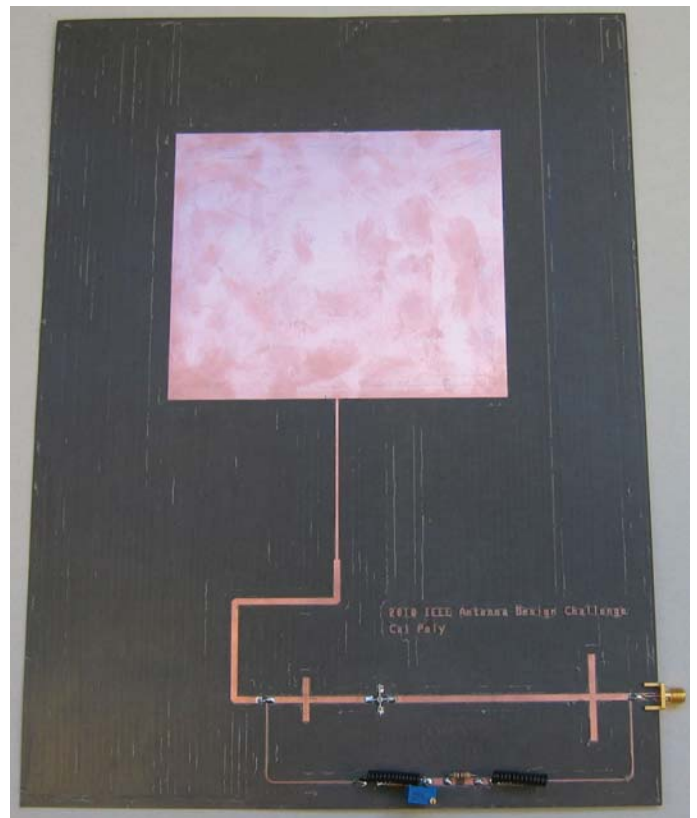


Figure 6. The embedded patch antenna illustrated an actual application (cell phones), and emphasized the benefits of microstrip antennas.

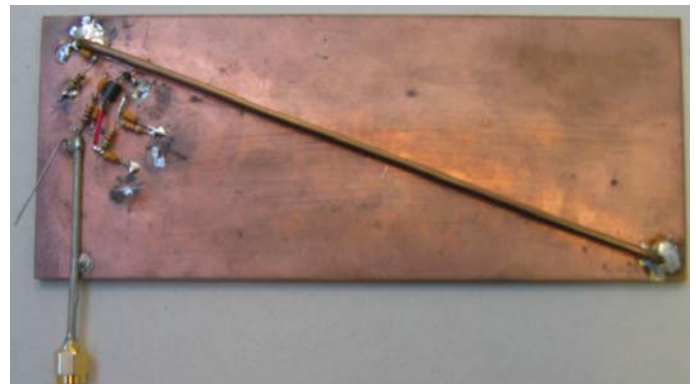


Figure 7. A negative-resistance oscillator provided the 915 MHz transmitted signal.

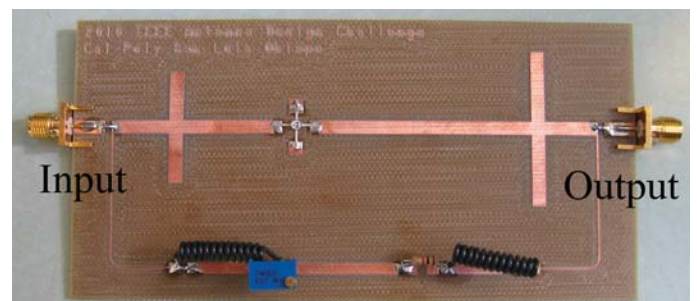
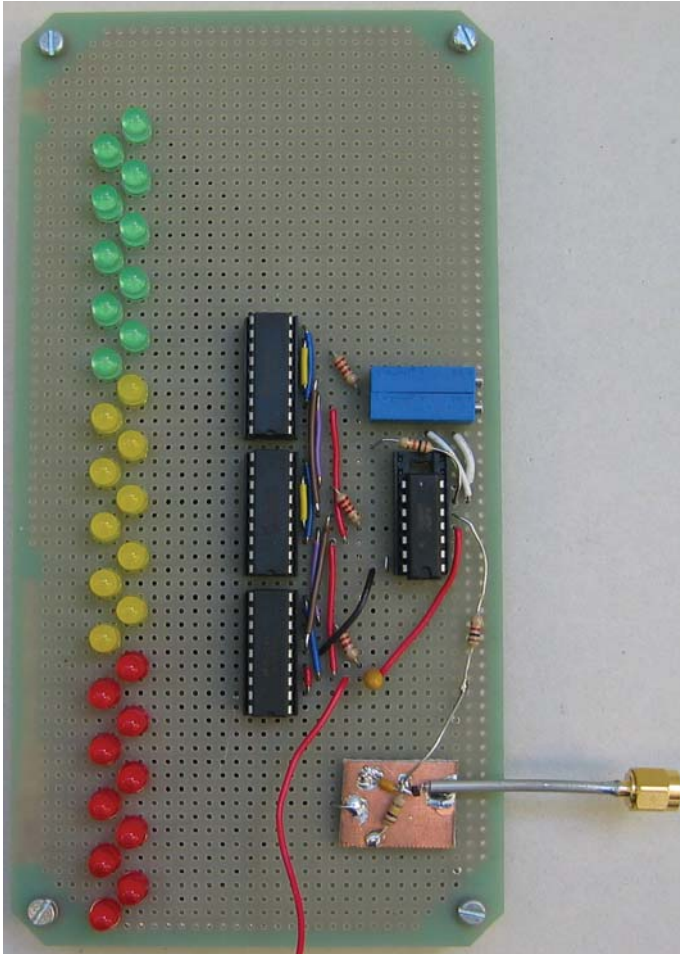


Figure 8. A microstrip amplifier provided 15 dB of signal gain.



**Figure 9.** A bandpass filter suppressed out-of-band transmissions.



**Figure 10.** The signal-strength indicator illuminated LEDs in proportion to the received RF signal strength.

copper mesh (see Figure 11). The drywall and poultry net represented building walls, while the ESD and copper mesh frames simulated electronics-manufacturing environments. EM wave attenuation caused by these conductive and metallic surfaces were illustrated by the system.

### 3. Assembly

#### 3.1 Dipole Elements

The dipole antennas used in the stationary, rotating, and corner-reflector antennas were all composed of 3/8 in outer-diameter and 5/32 in inner-diameter brass tubing, 10 AWG copper wire, and RG174 SMA male coaxial cable. Two 8.2 cm long slots ( $\lambda/4$  at 915 MHz) were cut into the 3/8 in brass tubing using a Dremel cutting-wheel attachment to form a split balun. 1/8 in diameter holes were drilled at one end of both

the 3/8 in and 5/32 in brass tubes to accommodate the dipole arms. The 10 AWG copper-wire dipole arms were soldered into the 1/8 in holes (see Figure 12). The initial 4 in length dipole arms were tuned by trimming 1/32 in increments from each arm

until  $|S_{11}|$  was minimized at 915 MHz. The input matching for the corner-reflector dipole is shown in Figure 13. Hot glue was applied inside the dipole's end to mechanically stabilize the tip of the split balun.

The coaxial feed line was stripped and the center conductor was soldered to the 5/32 in inner brass tube, whereas the outer coaxial conductor was soldered to the 3/8 in outer brass tube. The coaxial feed lines were approximately 2 ft long for the stationary and rotating dipole antennas, and approximately 3 ft long for the corner reflector. The stationary and rotating dipole-antenna tubing was 7 in long; the corner-reflector tubing was 20 in long.

#### 3.2 Stationary Dipole Antenna

The stationary dipole base was composed of wooden components secured with wood glue. All dimensions are defined in Figure 14. The mounting post was composed of two 1 in thick, 2 in wide posts, glued together as shown in Figure 14. A 17/32 in diameter hole accommodated the dipole.



**Figure 11.** Environmental barriers simulated actual wireless-system environments: (l-r) ESD, drywall, copper mesh, and poultry-net barriers.



**Figure 12.** The corner reflector dipole's input matching.

### 3.3 Rotating Dipole Antenna

The rotating dipole base was also composed of wooden components assembled using wood glue, except for the two lazy Susans, which were secured by wood screws. All dimensions are defined in Figure 15. A 17/32 in hole accommodated the dipole.

### 3.4 Corner Reflector

The corner-reflector table was composed of wood. All dimensions are defined in Figure 16. The corner-reflector table included slots that allowed 90°, 60°, or 30° corner-reflector angles. The 22 in × 22 in platform was attached to a 10 in × 22 in wooden base via a lazy Susan. Cable-tie mounts and cable ties secured the dipole and allowed dipole repositioning with the different corner angles (see Figure 17). For a 90° corner, the dipole was placed approximately 7.09 in from the corner's apex to achieve peak received field strength. The dipole was placed 8.39 in and 15.16 in from the corner's apex for the 60° and 30° corner angles, respectively.

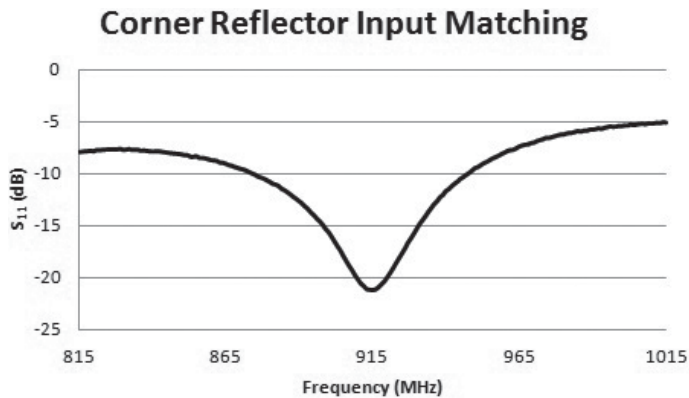


Figure 13. The dipole elements were supported by the split balun.

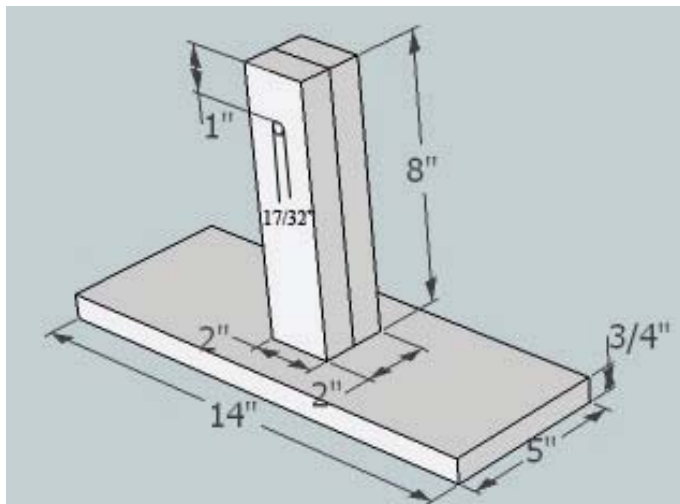


Figure 14. The base dimensions of the stationary dipole.

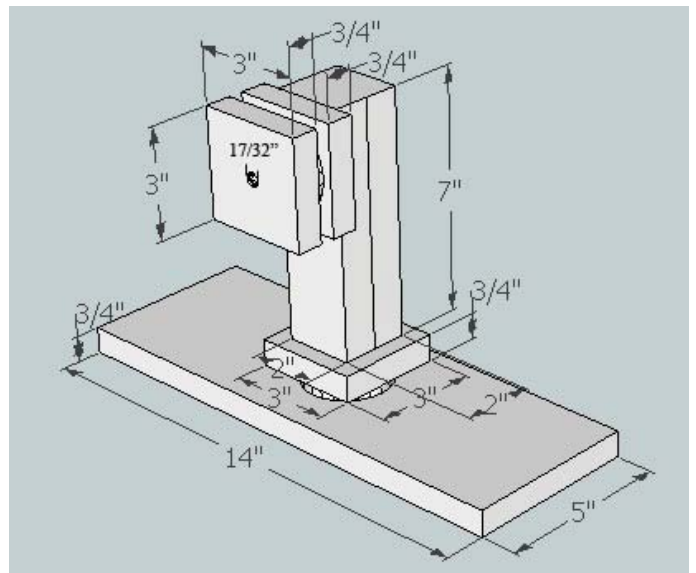


Figure 15. The base dimensions of the rotating dipole.

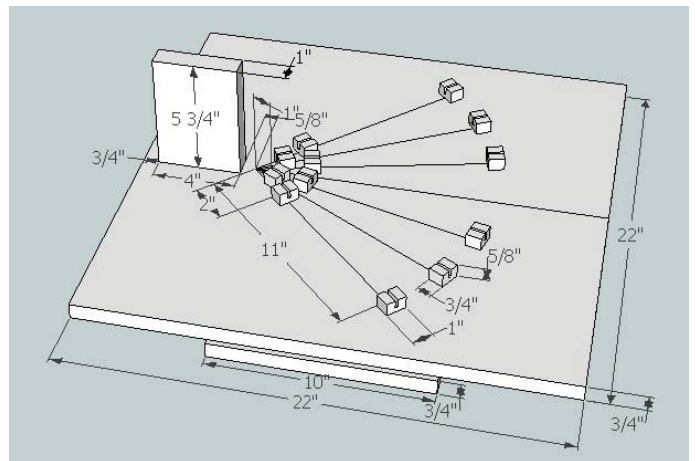


Figure 16. The dimensions of the corner reflector.



Figure 17. The dipole mount for the corner reflector.

### 3.5 Quagi Antenna

The Quagi antenna was composed of wood, a 5/16 in wooden dowel, and wood glue. All dimensions are defined in Figure 19. The boom was secured to the stand using a 5/16 in wooden dowel.

The Quagi elements were squares formed from 10 AWG solid copper wire. The directors, driven elements, and reflector

had 3.08 in, 3.23 in, and 3.43 in sides, respectively. The reflector and directors were soldered together to form closed squares. The driven element was fed by RG174 coax on the vertical side, to vertically polarize the antenna (see Figure 20).

The Quagi might also have required tuning. The driven element's unconnected side was initially 0.2 in longer than specified. On end of the driven element was filed down until  $|S_{11}|$  was minimized at 915 MHz. The Quagi's input matching is shown in Figure 18. A 1/32 in gap was maintained between the copper ends.

### 3.6 Embedded PCB Patch Antenna

The embedded PCB patch antenna was milled on 31-mil-thick, 9 in  $\times$  12 in RT Duroid 5870 laminate. The amplifier was similar to the FR4 amplifiers, and had the same biasing circuit. The PCB patch antenna's Gerber file is available upon request from the authors. The layout is shown in Figure 21.

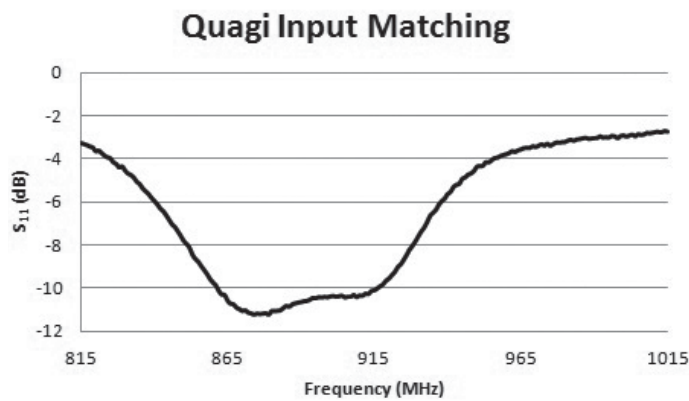


Figure 18. The Quagi's input matching.

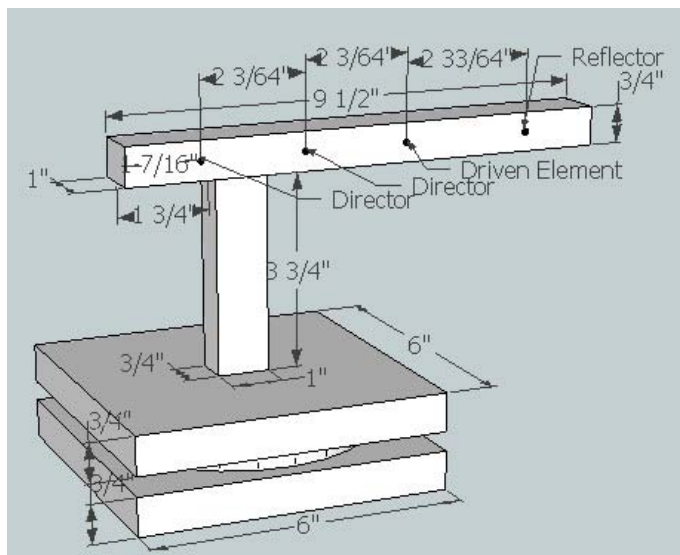


Figure 19. The dimensions of the Quagi antenna.



Figure 20. The Quagi was fed on the vertical side by a coaxial cable. The gap length was 1/32 in.

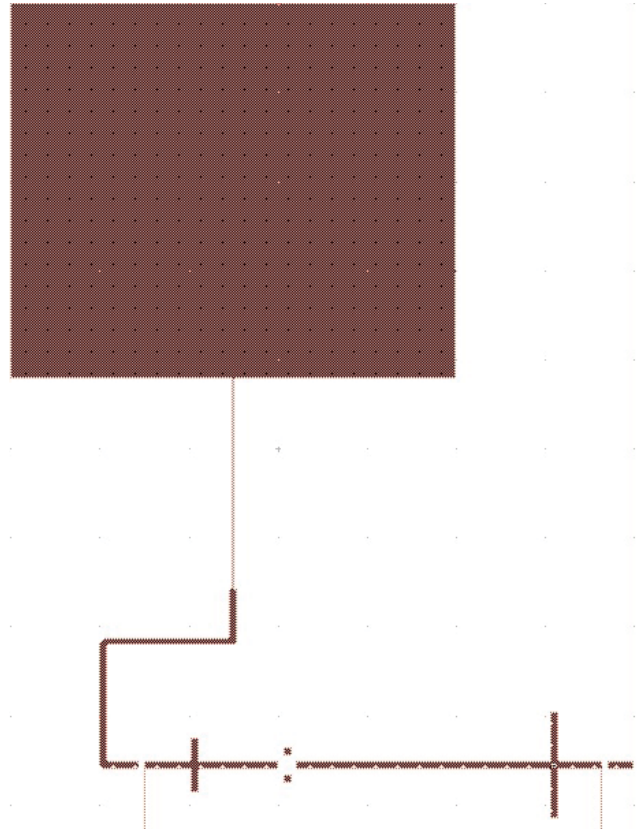


Figure 21. The layout of the embedded PCB patch antenna.

### 3.7 Oscillator

The oscillator was assembled on 62 mil FR4 laminate. The schematic is given in Figure 22. Resonance occurred in a  $\lambda/2$  (6.38 in) 10 AWG solid copper wire. The copper-wire resonator was applied to the Avago AT-41486 transistor's emitter lead. The coupled wire was positioned between the resonator and the ground plane at one end of the resonator (see Figure 23). The copper wire rested approximately 2 mm above the ground plane. The oscillator required 9 V dc.

The oscillator operated on the principle of negative resistance, an unstable condition to initiate oscillation. As the signal amplitude increased, the negative-resistance value decreased to stabilize the RF signal. To create a negative input resistance,

an inductance was required at the transistor's base. Sufficient inductance at the transistor's base was achieved using a minimum 0.5-in-long lead (see Figure 22).

The oscillation frequency was dependent on the copper-wire resonator's length and the copper wire's height above the ground plane. The oscillation frequency was adjusted by altering the resonator's height.

### 3.8 Amplifiers

The amplifiers were milled on 62 mil thick, 2.5 in × 5 in FR4 laminate (see Figure 24). The board included traces for dc biasing the AT-41435G RF transistor, and solder pads for dc biasing. The biasing circuit was shorted to ground with a via  $\lambda/4$  away from the RF transmission line to create an ac open circuit near the RF transmission line (see Figure 24). The handmade 50 nH inductors were composed of 24 AWG wire, formed into 13 0.1-in-diameter loops, and were 0.7 in long. A magnified view of the biasing circuitry is shown in Figure 25, and the biasing schematic is shown in Figure 26.

The amplifiers required 5 V dc input voltage applied to the collector. The base-emitter junction was biased by adjusting the potentiometer's resistance,  $R1$ , which was directly proportional to the voltage drop. This voltage was applied to the transistor base. The potentiometer's resistance was increased to give 0.7 V.

### 3.9 Bandpass Filters

The bandpass filter was milled on 31-mil-thick, 1-in × 7.75-in RT Duroid 5870 laminate. The coupled-line bandpass filter Gerber file is available upon request from the authors. The bandpass filter's dimensions are given in Figure 27.

### 3.10 Signal-Strength Indicator

The signal-strength indicator schematic is shown in Figure 28. Schottky diodes, 1000 pF capacitor  $C1$ , and 100 k $\Omega$  resistor  $R1$  were soldered to a 1 in × 1 in FR4 panel. The remaining circuit components were soldered onto vectorboard, which was mounted onto FR4. The signal-strength detector required 6 V dc.

The signal detector included a non-inverting op amp to adjust the detected peak voltage range. The gain was adjusted by increasing the feedback-potentiometer's resistance,  $R1$ .

## 4. Operation

### 4.1 System Setup

Locate an open workspace to allow for (3 ft) antenna separation. Allow space for dc power supplies, and remove

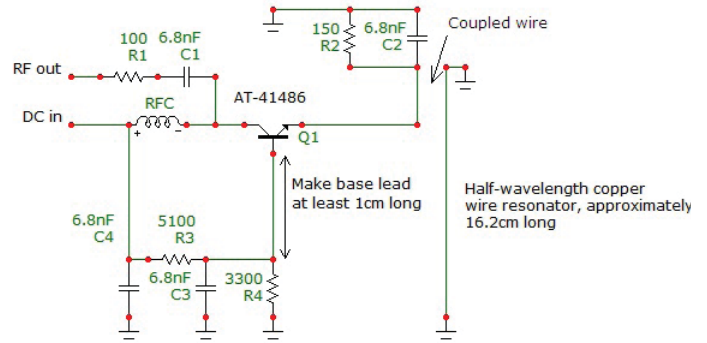


Figure 22. The schematic of the oscillator.



Figure 23. The coupling between the transistor and the copper-wire resonator.

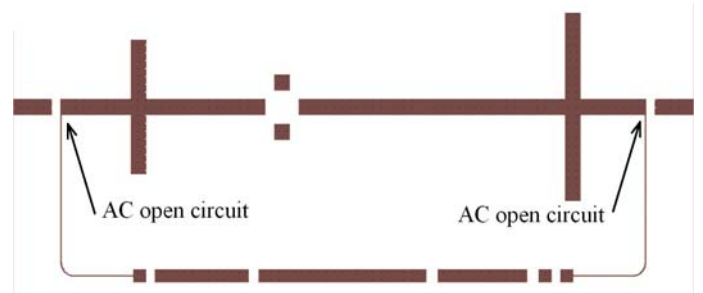


Figure 24. The layout of the 915 MHz amplifier.



Figure 25. The amplifier's bias circuit.

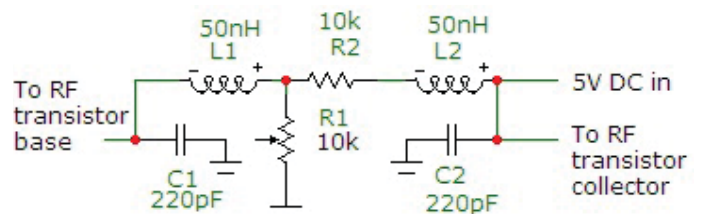


Figure 26. The schematic showing the amplifier's biasing.

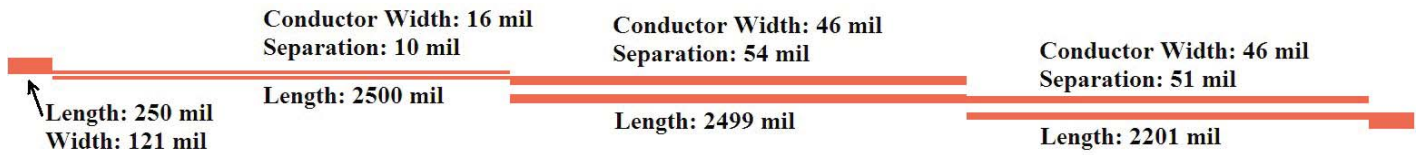


Figure 27. The layout of the bandpass filter.

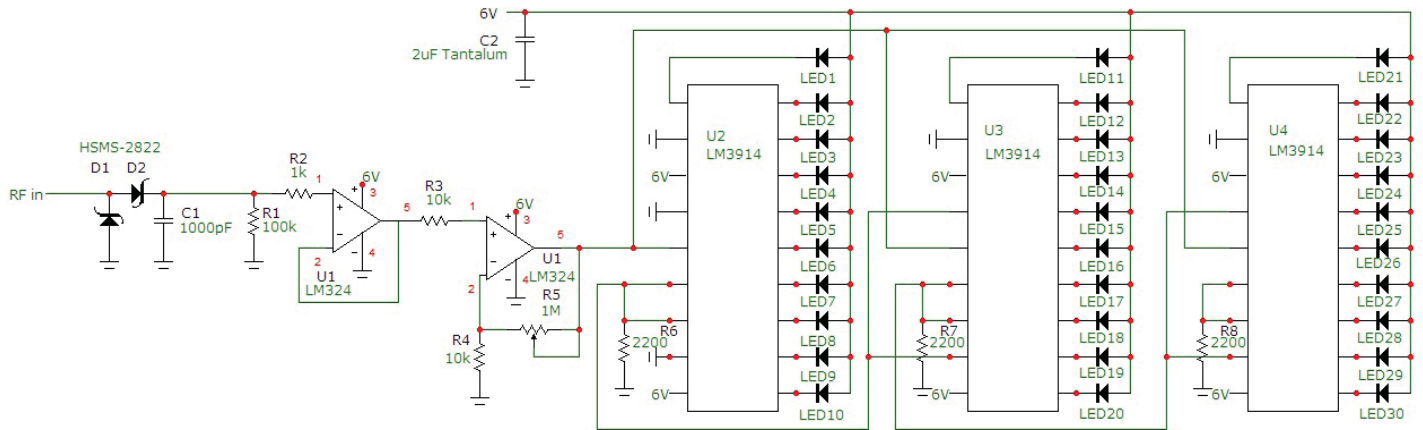


Figure 28. The signal-strength detector was comprised of Schottky diodes, LM3914 bar-graph displays, op amps, and passive components.

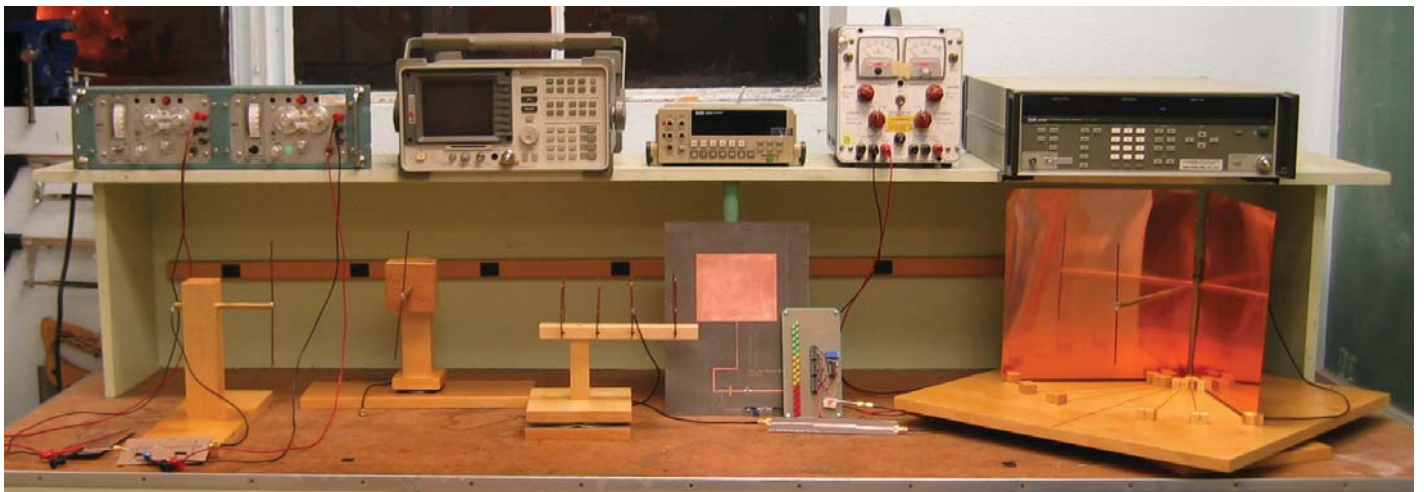


Figure 29. The complete demonstration system. For reference, the bench was 7 ft across.

large conductive objects to minimize reflections. Interconnect the oscillator, amplifier, and stationary dipole using SMA cables. Apply 9 V dc and 6 V dc to the oscillator and signal-strength indicator. Set the amplifier potentiometer to 0  $\Omega$ , and apply 5 V to the collector's bias port. Increase the potentiometer's resistance until the base port reaches 0.7 V.

Locate the rotating dipole antenna 3 ft from the stationary dipole, positioning it as seen in Figure 3. Connect the rotating dipole antenna to the bandpass filter and signal-strength detector. Increase the signal detector's gain by increasing the resistance of the potentiometer until all LEDs are illuminated. If maximum gain is applied and all 30 LEDs are not illuminated, reduce the gain to zero by decreasing the resistance of  $R_5$  to 0  $\Omega$

and inserting the second RF amplifier between the receiving antenna and the bandpass filter. Increase the signal-strength detector's gain until all 30 LEDs are illuminated. The system is now ready for demonstration.

## 4.2 Rotating Dipole

The first demonstration uses the rotating dipole to demonstrate signal reception, radiation patterns, and antenna-pattern nulls. With all 30 LEDs illuminated, adjust the roll of the rotating antenna to demonstrate polarization effects on received signal strength. Adjust the roll 90° for minimum reception (see Figure 3 for roll direction).



To demonstrate dipole-antenna radiation-pattern nulls, position the rotating dipole as depicted in Figure 3. Rotate the antenna by 90° in both the roll and azimuth. The tip of the dipole should be pointing at the transmitting antenna. When oriented this way, there should be no signal strength observed on the signal-strength detector.

Spreading loss is demonstrated by increasing the distance between the transmitting and receiving antennas to 5 ft.

### 4.3 Corner Reflector

The corner reflector demonstrates antenna arrays and radiation-pattern effects. Begin without the corner. Adjust the azimuth by 90° (azimuthal direction indicated in Figure 16), and observe signal-strength variation. Introduce the 90° corner and adjust the azimuth. Observe how the signal-strength variation differs. Repeat the procedure with a 60° and 30° corner angle. For 90°, 60°, and 30° corners, 60°, 40°, and 20° H-plane half-power beamwidths (HPBW) are expected, respectively.

### 4.4 Quagi

The Quagi antenna demonstrates a directional antenna and the resultant radiation patterns. Begin by directing the main beam toward the transmitting antenna. Observe the difference in signal strength between the Quagi and the other antennas. Slowly rotate the Quagi, and observe the Quagi's main-beam angular dependence on received signal strength. The expected H-plane half-power beamwidth is 40°.

### 4.5 Embedded PCB Patch Antenna

The embedded PCB patch antenna demonstrates modern antenna-fabrication methods. The antenna was milled adjacent to RF circuitry on the same PCB. If a flexible laminate is used, the antenna can conform to non-planar surfaces.

Begin by biasing the amplifier per Section 4.1. Locate the patch antenna 3 ft from the transmitting antenna. Observe the radiation pattern by rotating the patch antenna in the azimuthal direction. The expected H-plane half-power beamwidth is 60°.

### 4.6 Environmental Barriers

The environmental barriers can be used in conjunction with any of the first four demonstrations. Placing the barriers midway between the transmitting and receiving antennas (far zone) demonstrates effects on received signal strength.

Because the ESD bags, copper mesh, and poultry net are composed of metallic components, large signal attenuation occurs. Because the copper mesh holes are much less than

$\lambda/10$  (1.26 in) in diameter, the most attenuation occurs with copper mesh. Because the poultry-net hole diameter is on the order of  $\lambda/10$ , less attenuation is noted.

## 5. Conclusion

The wireless system can successfully demonstrate many antenna characteristics with minimal required support instrumentation (a dc power supply). Polarization, radiation pattern, gain, and barrier-induced signal-attenuation effects can be illustrated for four antenna types: dipole, corner reflector, Quagi, and embedded patch. These represent dominant antenna types used in current applications.

Visual indication of received signal strength is provided by an LED array, driven by an RF peak detector and low-pass filter. All receiving antennas were mounted onto rotational platforms, to allow investigation of radiation-pattern and polarization effects. Student-designed and fabricated components – an RF oscillator, amplifiers, and filters – complement the wireless system, and reduce external support instrumentation requirements.

The combined parts and services required to build the entire system totaled less than \$900 (Table 1). The entire system can be assembled in as little as four weeks with proper equipment.

## 6. Acknowledgment

The authors would like to thank Dr. Dennis Derickson for assistance with the oscillator, RF peak detector, and Quagi antenna. They would like to thank Mr. Daniel Hempy for advice and assistance with the design and construction of the antenna-support structures.

## 7. References

1. W. Stutzman and G. Thiele, *Antenna Theory and Design, Second Edition*, New York, John Wiley and Sons, Inc., 1998.
2. J.-S. Hong and M. J. Lancaster, *Microstrip Filters for RF/Microwave Applications*, New York, John Wiley and Sons, Inc., 2001.
3. D. M. Pozar, *Microwave and RF Design of Wireless Systems*, New York, John Wiley and Sons, Inc., 2001.
4. R. Douville and D. James, "Experimental Study of Symmetric Microstrip Bends and their Compensation," *IEEE Transactions on Microwave Theory and Techniques*, **MTT-26**, 3, March 1978.
5. "Voltage Multipliers," available online at [http://www.allaboutcircuits.com/vol\\_3/chpt\\_3/8.html](http://www.allaboutcircuits.com/vol_3/chpt_3/8.html).

**Table 1. The list of parts for the demonstration system.**

Part	Est. Cost (\$)	Qty.	Total Cost	Mfr. Part Number	Vendor
<b>Misc. Parts</b>					
1" thick wood	10.00	2 sq. ft	\$10.00		Local hardware store
3/4" thick wood	40.00	12 sq. ft	40.00		Local hardware store
Misc. Resistor Pack	9.95	1	9.95	ASST8-R	www.jameco.com
31mil SMA edge connectors	5.45	3	16.35	142-0701-881	www.mouser.com
62mil SMA edge connectors	3.70	4	14.80	132255	www.mouser.com
Rogers RT Duroid 31 mil thick 5870 9" x 12"	50.00	2	100.00		www.rogerscorp.com
15cm x 15 cm FR4 PCB	5.95	1	5.95	21-221-R	www.jameco.com
30' 10AWG solid copper wire	15.00	1	15.00		Local hardware store
SMA male male connectors	2.95	2	5.90	S-311-G-R	www.jameco.com
3' of 3/8" diameter brass tubing	6.99	2	13.98		Local hobby store
3' of 5/32" diameter brass tubing	3.19	2	6.38		Local hobby store
4' RG174 SMA male male coax	7.58	2	15.16	CO-174SMAX200	COD <sup>1</sup>
2' RG174 SMA male male coax	7.10	1	7.10	CO-174SMAX200	COD <sup>1</sup>
Misc. screws, nails, wood glue	10.00	1	10.00		Local hardware store
0.0865" semi-rigid coax, 1ft	24.62	1	24.62	UT-85-TP-M17	MSI <sup>2</sup>
SMA straight plug 0.085" connector	2.32	2	4.64	132101	www.mouser.com
PCB fabrication, four PCBs	400.00	1	400.00		www.hughescircuits.com
<b>Rotating Dipole Antenna</b>					
3" x 3" Lazy Susan bearing	1.50	2	\$3.00		Local hardware store
<b>Corner Reflector Antenna</b>					
6" x 6" Lazy Susan bearing	3.50	2	\$7.00		Local hardware store
16 mil, 12" square copper sheets (2)	39.99	1	39.99		www.basiccopper.com
<b>Quagi Antenna</b>					
5/16" diameter 2" long wood dowel	0.20	1	\$0.20		Local hardware store
<b>Oscillator</b>					
Avago AT-41486 transistor	2.59	1	\$2.59	AT-41486-BLKG	www.digikey.com
6800pF capacitor	0.22	5	1.10	C410C682K1R5TA7200	www.digikey.com
RF choke	0.12	1	0.12	BL01RN1A1D2B	www.mouser.com
<b>Amplifiers (x2)</b>					
Avago AT-41435G transistor	5.00	3	\$15.00	AT-41435G	www.avnet.com
220pF SMT capacitor	0.05	12	0.60	06035A221J4T2A	www.jameco.com
25 turn 0.5W 10kΩ potentiometer	1.95	3	5.85	3299W-1-103VP	www.jameco.com
<b>Signal Strength Indicator</b>					
HSMS-2822 Schottky diode	0.67	1	\$0.67	HSMS-2822-BLKG	www.jameco.com
LM3914N-1 linear bar graph driver	1.95	3	5.85	LM3914N-1	www.jameco.com
Protoboard	13.95	1	13.95	2852PCB-R	www.jameco.com
Mounting hardware kit	2.95	1	2.95	106551	www.jameco.com
Green LEDs	0.10	10	1.00	LG13740	www.jameco.com
Yellow LEDs	0.15	10	1.50	LY3330	www.jameco.com
Red LEDs	0.11	10	1.10	LTL-307E	www.jameco.com
LM324N operational amplifier	0.29	1	0.29	LM324N	www.jameco.com
18 pin IC socket	0.14	4	0.56	CA-18SDL-1T	www.jameco.com
1000pF capacitor	0.12	1	0.12	SA105A102JAA	www.jameco.com

<sup>1</sup>COD: www.cablesondemand.com

<sup>2</sup>MSI: www.microstock-inc.com

**Table 1. The list of parts for the demonstration system (continued).**

Part	Est. Cost (\$)	Qty.	Total Cost	Mfr. Part Number	Vendor
<b>Environmental Barrier</b>					
1/2" × 3/4" pine, 1' length	0.74	24	17.76		Local hardware store
2' × 2', 0.5" thick drywall	3.98	1	3.98		Local hardware store
6" × 10" ESD bags (100 ct)	13.40	1	13.40	48602	www.mouser.com
2' wide poultry net	5.88	1	5.88		Local hardware store
Copper Mesh #60 X 60 .0075" 24" × 24"	22.90	1	22.90		www.amazon.com
8' long 0.5" PVC pipe	1.16	2	2.32		Local hardware store
0.5" diameter PVC tee	0.29	4	1.16		Local hardware store
0.5" diameter PVC 90° corner	0.22	2	0.44		Local hardware store
0.5" diameter PVC end cap	0.25	4	1.00		Local hardware store

6. National Semiconductor LM3914 Datasheet, National Semiconductor, Santa Clara, CA, 2003.

7. ARRL, *The ARRL Antenna Book, 21st Edition*, Newington, CT, ARRL, Inc., 2007.

8. R. C. Jaeger and T. N. Blalock, *Microelectronic Circuit Design, Second Edition*, New York, McGraw-Hill, 2004.

9. G. Elmore. "Designing a Station for the Microwave Bands: Part 2," *Ham Radio Magazine*, October 1988, pp. 19-31.

10. C. A. Balanis, *Antenna Theory Analysis and Design, Third Edition*, New York, John Wiley and Sons, Inc., 2005.

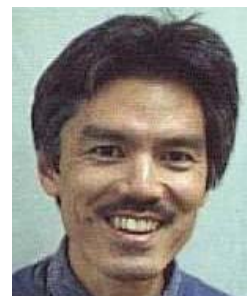


**Mike Civerolo** is an Electrical Engineer at SPAWAR Systems Center Pacific. He received his BSEE and MSEE from California Polytechnic State University, San Luis Obispo. He lives in San Diego, CA, with his wife, Jacqueline.

## Introducing the Authors



**Alex Hempy** is an Antenna and Microwave Engineer at Raytheon Company, Goleta, CA. He received the BSEE and MSEE degrees from California Polytechnic State University, San Luis Obispo, in June 2010.



**Dean Arakaki** is an Associate Professor in the Electrical Engineering Department at California Polytechnic State University, San Luis Obispo. He teaches courses in the electromagnetics, RF systems, and antenna areas. He received the BSEE from California State Polytechnic University, Pomona; the MBA and MSEE from California State University, Long Beach; and the PhD in Electrical Engineering from the Pennsylvania State University, University Park, PA. 